Title

Communication—O3-Type Layered Oxide with a Quaternary Transition Metal Composition for Na-Ion Battery Cathodes: NaTi0.25Fe0.25Co0.25Ni0.25O2

Journal

Journal of The Electrochemical Society, 164(14)

ISSN

0013-4651

Authors

Vassilaras, Plousia
Dacek, Stephen T
Kim, Haegyeom
et al.

Publication Date

2017

DOI

10.1149/2.0271714jes

Peer reviewed

Communication—O3-Type Layered Oxide with a Quaternary Transition Metal Composition for Na-Ion Battery Cathodes: $NaTi_{0.25}Fe_{0.25}Co_{0.25}Ni_{0.25}O_2$

Plousia Vassilaras,[a] Stephen T. Dacek,[a] Haegyeom Kim,[b,*] Timothy T. Fister,[c] Soojeong Kim,[c] Gerbrand Ceder,[a,b,*] and Jae Chul Kim[b,z]

[a]*Department of Materials Science and Engineering, Massachusetts Institute of Technology, Cambridge, Massachusetts 02139, USA*
[b]*Materials Sciences Division, Lawrence Berkeley National Laboratory, Berkeley, California 94720, USA*
[c]*Chemical Sciences and Engineering Division, Argonne National Laboratory, Argonne, Illinois 60439, USA*

$NaTi_{0.25}Fe_{0.25}Co_{0.25}Ni_{0.25}O_2$ is explored as a cathode material for Na-ion batteries. Synthesized by a solid-state reaction, the compound is phase-pure with the O3-type layered structure and consists of Ti^{4+}, Fe^{3+}, Co^{3+}, and Ni^{2+} according to X-ray absorption spectroscopy. The cathode delivers 163 mAh/g and 504 Wh/kg at C/20 in the first discharge with 89% capacity retention after 20 cycles and demonstrates superior rate capability with micron sized particles, in which discharge capacity at 30 C is 80 mAh/g. Our results indicate that the Ti-containing quaternary material can be a potential cathode composition for Na-ion batteries.

Manuscript submitted July 10, 2017; revised manuscript received September 14, 2017. Published November 11, 2017.

Rechargeable batteries that reversibly cycle Na ions are a cost-effective alternative to the Li-based technology to meet increasing demand and need for grid-level energy storage.[1] Unlike Li cathode chemistries that heavily rely on Co and Ni, Na-intercalating oxides tend to form energy-dense layered structures with almost all transition metals including Cu,[2–4] allowing a broad selection and combination of redox centers to tune electrochemical properties and air-stability. In particular, Fe is an attractive metal due to its high redox potential and natural abundance.[5] However, the performance of layered $NaFeO_2$ as a cathode is impractical; Fe^{4+} migration upon desodiation destabilizes the structure, leading to poor Na ion mobility and irreversibility.[6]

The charged state stability of the layered structure, and thereby their electrochemical properties,[7] can be enhanced by partially substituting Fe into redox-inactive elements and/or other transition metals.[8–11] Li et al. proposed an optimal Fe content ($< \sim 33\%$) that promotes Na diffusion at the high state of charge.[12,13] Here, we use Ti^{4+} as a structural stabilizer and report an O3-type[14] Na transition metal oxide (O3-Na**M**O_2) composition, $NaTi_{0.25}Fe_{0.25}Co_{0.25}Ni_{0.25}O_2$ (TFCN), for the optimized Fe redox activity. Our results demonstrate a substantial amount of reversible Na intercalation and high rate capability of TFCN, implying that the material may be successfully used as a Na-ion battery cathode.

Methods

A stoichiometric amount of transition metal precursors (TiO_2, Fe_2O_3, Co_3O_4, and $NiCO_3$, all from Sigma-Aldrich) were mixed with 20% excess Na_2O (Sigma-Aldrich) by planetary ballmilling at 500 rpm for 4 hours. The resulting mixture was fired at 900°C for 12 hours under flowing O_2, quenched to room temperature, and transferred to an Ar-filled glove box to prevent air-exposure. The crystal structure and particle morphology of as-prepared TFCN were analyzed by X-ray diffraction (XRD, PANalytical X'Pert Pro) with Rietveld refinement and scanning electron microscopy (SEM, Zeiss Merlin), respectively. Transition metal oxidation states were probed by X-ray absorption spectroscopy (XAS) obtained at Advanced Photon Source (13ID-E) in Argonne National Laboratory. For half-cell tests, cathodes were prepared by mixing the active material, Super P (Timcal) carbon, and polytetrafluoroethylene (Dupont) binder in a weight ratio of 80:15:5. Na metal (Sigma-Aldrich) was used as anodes. Electrolytes were prepared by dissolving 1 M $NaPF_6$ into ethylene carbonate:diethylcarbonate (1:1 by volume, BASF). Swagelok cells with a loading density of $\sim$2.4 mg/cm^2 were assembled using glass fiber (Whatman, GF/F) separators. The cells were cycled (1C = 242 mA/g) at room temperature using a Solartron 1470E potentiostat.

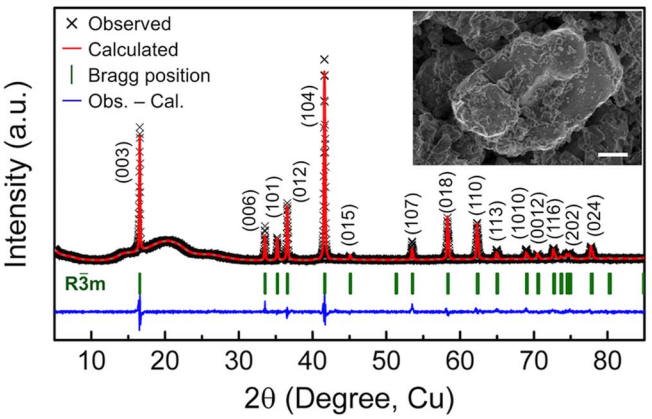

Figure 1. Rietveld-refined XRD pattern and SEM image (inset, scale bar: 2 μm) obtained from as-prepared TFCN. Background humps are due to a sealing Kapton film. $R_{wp} = 2.6967$, $R_p = 1.6841$, $\chi^2 = 5.9666$.

Results

Figure 1 shows XRD and Rietveld refined profile of TFCN. The material is phase-pure, and all peaks indexed exhibit the $R\bar{3}\,m$ symmetry, corresponding to the O3 structure. Refinement yields the hexagonal lattice with $a_{hex} = 2.9768(5)$ Å and $c_{hex} = 16.012(4)$ Å, as summarized in Table S1 (Supplemental Material). In accordance with Vegard's rule, the obtained structural parameters agree with values interpolated from O3-$NaTi_{0.5}Ni_{0.5}O_2$,[15] O3-$NaCoO_2$,[16] and O3-$NaFeO_2$.[17] The average particle size of TFCN, as determined by SEM, is $\sim$3 μm but we also observe particles up to 10 μm, as shown in the inset.

XAS were collected to identify oxidation states of the transition metals in as-synthesized TFCN. Ti is determined to be tetravalent as its K-edge aligns with a TiO_2 reference in Figure 2a. The edges of Fe and Co closely match those of Fe_2O_3 and $LiCoO_2$ in Figure 2b and 2c, respectively, suggesting that they occupy a trivalent state. Ni is divalent, as compared with a reference edge from NiO in Figure 2d. The XAS result suggests that Ti likely remains inert while other transition metals can be redox-active upon cycling.

*Electrochemical Society Member.
[z]E-mail: jckim@lbl.gov

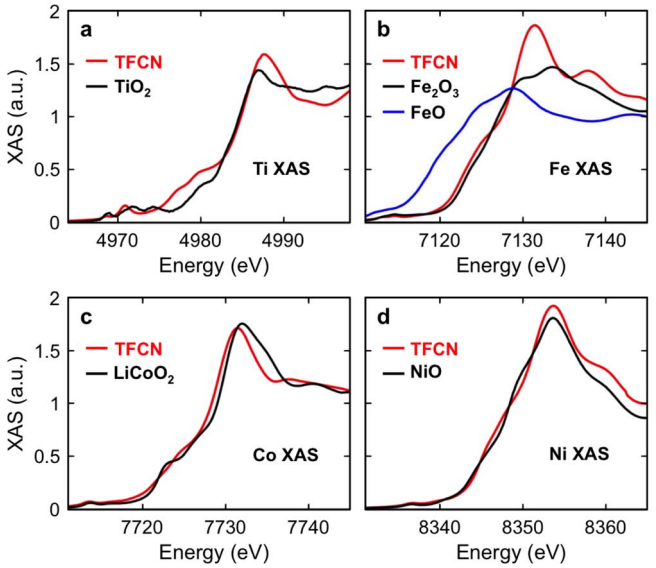

Figure 2. XAS (K-edge) from (a) Ti, (b) Co, (c) Fe, and (d) Ni of TFCN.

Figure 3a shows voltage profiles of TFCN as a function of specific capacity in a 2–4 V window at C/20. A plateau is present in the voltage profile at ∼2.8 V (Na∼0.75). Charge/discharge capacities at the first, second, and twentieth cycles are 163/145, 147/144, and 130/129 mAh/g, respectively. Compared with results first reported by Yue et al.,[18] we obtain improved capacity at this rate, which may result from different electrode preparation methods and/or electrolytes used. An average decay rate of the discharge capacity plotted in Figure 3b is 0.55% per cycle. To investigate how the voltage range affects the overall performance of TFCN, a new charge cutoff is set at 4.2 V. As shown in Figure 3c, it leads to larger discharge capacities: 177/163, 163/160, and 149/146 mAh/g in the first, second, and twentieth charge/discharge, respectively. An additional plateau-like feature at ∼4.1 V is found in the first charge but unobservable in the subsequent discharge cycle. The plateau reappears in the second charge and gradually vanishes in further cycles. The average rate of discharge capacity fade is 0.52% per cycle when cycled in 2–4.2 V (Figure 3d).

We further tested the discharge rate capability of TFCN in 2–4.2 V, and Figure 4a shows the voltage–capacity profiles. The cell delivers 163, 158, 153, 141, 123, and 111 mAh/g at C/20, C/10, C/5, 1 C, 5 C, and 10 C, respectively. Remarkably, the capacities achieved at 20 C and 30 C are 95 and 80 mAh/g, respectively, demonstrating high rate performance despite the very large particle size. In Figure 4b, specific energies of TFCN achieved in 2–4.2 V as a function of the C-rate are plotted with those of other O3-Na**M**O_2 for comparison.[4,9,10,19–21] TFCN indeed exhibits superior electrochemical performance: the specific energies achieved are 504 Wh/kg at C/20 and 200 Wh/kg at 30 C, outperforming many O3-Na**M**O_2 compounds.

Discussion

Na content strongly affects the phase stability of O3-Na**M**O_2,[2] in which desodiation typically induces phase transition to a P3-type[14] structure that is stable between $0.5 < Na < 0.8$.[22] This is a reversible first-order phase transformation that produces a voltage plateau with respect to the capacity, as shown by ex situ XRD in Figure S1 and also commonly observed in O3-Na**M**O_2.[1] When desodiated beyond Na ∼0.3, the P3-structure may undergo another phase transition that is usually accompanied by an abruptly decreasing *c*-lattice parameter, leading to either a reversible P3-O3(-O1) phase transformation or irreversible Fe^{4+} migration in Fe-containing compositions.[8,13,22,23] Fe^{4+} in this compound was observed by Yue et al.,[18] and other work also showed oxidation of Fe^{3+} to Fe^{4+} below 4 V.[6,8,13] We found the latter in Figure S1. Thus, the reversible and irreversible plateaus at 2.8 and

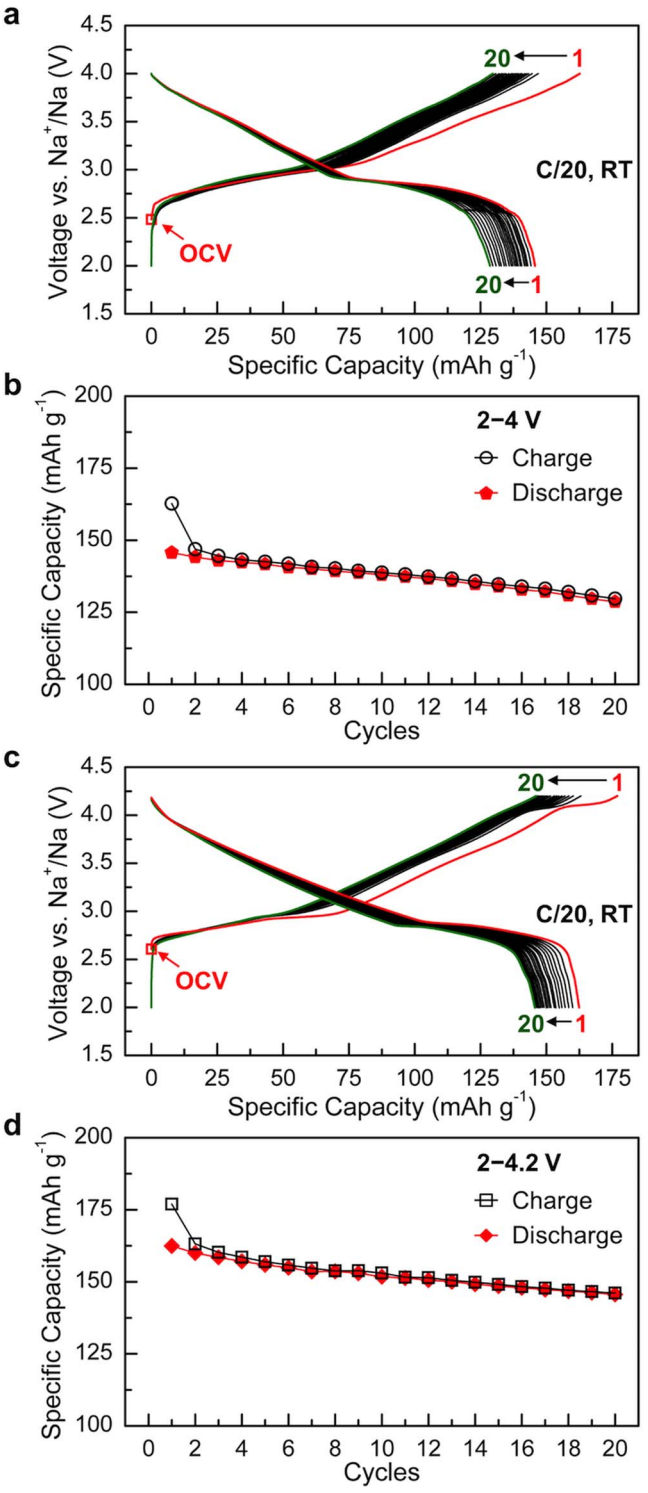

Figure 3. Voltage vs. capacity profiles and cyclability of TFCN in (a-b) 2–4 V and (c-d) 2–4.2 V.

4.1 V for TFCN in Figure 3c may originate from the O3-P3 transition and Fe^{4+} migration, respectively. However, how each transition metal individually contributes to the overall redox reaction and associated structural evolution is unclear at this point.

Na intercalation in Fe-containing Na_x**M**O_2 is very sensitive to the voltage cutoff (i.e., the stability of desodiated structures).[6] For TFCN, the capacity retention is independent of the voltage range in Figure 3. Moreover, the average capacity retention rate and coulombic

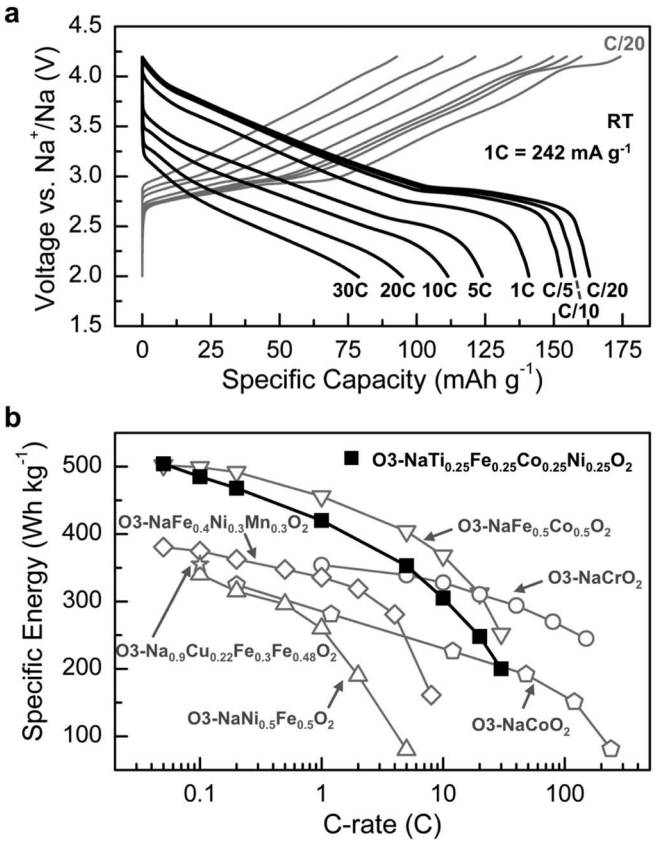

Figure 4. (a) Rate capability and (b) specific energy of TFCN as a function of C-rate compared to those of other O3-$NaMO_2$ cathode materials.[4,9,10,19–21]

efficiency of TFCN (89% and 98.5% at the 20th cycle, respectively) is higher than that of O3-$NaFe_{1/3}Co_{1/3}Ni_{1/3}O_2$ (84% and 97.3% at the 20th cycle, respectively) even though both materials have the same initial capacity.[24] Thus, Ti may partially stabilize the charged structure, resulting in improved electrochemical properties. Considering that particles of TFCN are micron-sized with random morphology, it is likely that its performance can be improved by further optimization. Therefore, our results suggest that Ti-containing layered compounds exhibit promising electrochemical properties. Moreover, this quaternary system can better tailor the performance of Na-ion batteries by having many different combinations of transition metals. In future work, we will further investigate the effect of Ti substitution on the layered structure and electrochemical properties.

Summary

The electrochemical properties of an O3-type layered sodium quaternary-mixed transition metal oxide, $NaTi_{0.25}Fe_{0.25}Co_{0.25}Ni_{0.25}O_2$, as a positive electrode material for rechargeable Na-ion batteries are demonstrated. The cathode delivers a substantial capacity and exhibits excellent rate capability. Our results show the potential of Ti-doped Na compounds to have high specific energy.

Acknowledgments

This work is financially supported by Samsung Advanced Institute of Technology. The Advanced Photon Source is supported by DOE (DE-AC02-06CH11357) and work at sector 13 is supported by NSF (EAR-1128799) and DOE (DE-FG02-94ER14466). Fister performed XAS measurements with support from DOE (DE-AC02-06CH11).

References

1. H. Kim, H. Kim, Z. Ding, M. H. Lee, K. Lim, G. Yoon, and K. Kang, *Adv. Energy Mater.*, **6**, 1600943 (2016).
2. S. Kim, X. Ma, S. P. Ong, and G. Ceder, *Phys. Chem. Chem. Phys.*, **14**, 15571 (2012).
3. S. Xu, X. Wu, Y. Li, Y.-S. Hu, and L. Chen, *Chin. Phys. B*, **23**, 118202 (2014).
4. L. Mu, S. Xu, Y. Li, Y.-S. Hu, H. Li, L. Chen, and X. Huang, *Adv. Mater.*, **27**, 6928 (2015).
5. P. Barpanda, *Chem. Mater.*, **28**, 1006 (2016).
6. N. Yabuuchi, H. Yoshida, and S. Komaba, *Electrochemistry*, **80**, 716 (2012).
7. Y.-N. Zhou, J. Ma, E. Hu, X. Yu, L. Gu, K.-W. Nam, L. Chen, Z. Wang, and X.-Q. Yang, *Nat. Commun.*, **5**, 5381 (2014).
8. J. S. Thorne, R. A. Dunlap, and M. N. Obrovac, *J. Electrochem. Soc.*, **160**, A361 (2013).
9. N. Yabuuchi, M. Yano, H. Yoshida, S. Kuze, and S. Komaba, *J. Electrochem. Soc.*, **160**, A3131 (2013).
10. P. Vassilaras, D.-H. Kwon, S. T. Dacek, T. Shi, D.-H. Seo, G. Ceder, and J. C. Kim, *J. Mater. Chem. A*, **5**, 4596 (2017).
11. J. S. Thorne, S. Chowdhury, R. A. Dunlap, and M. N. Obrovac, *J. Electrochem. Soc.*, **161**, A1801 (2014).
12. X. Li, D. Wu, Y.-N. Zhou, L. Liu, X.-Q. Yang, and G. Ceder, *Electrochem. Commun.*, **49**, 51 (2014).
13. X. Li, Y. Wang, D. Wu, L. Liu, S. H. Bo, and G. Ceder, *Chem. Mater.*, **28**, 6575 (2016).
14. C. Delmas, C. Fouassier, and P. Hagenmuller, *Physica B & C*, **99**, 81 (1980).
15. H. Yu, S. Guo, Y. Zhu, M. Ishida, and H. Zhou, *Chem. Commun.*, **50**, 457 (2014).
16. Y. Takahashi, Y. Gotoh, and J. Akimoto, *J Solid State Chem*, **172**, 22 (2003).
17. Y. Takeda, K. Nakahara, M. Nishijima, N. Imanishi, O. Yamamoto, M. Takano, and R. Kanno, *Mater. Res. Bull.*, **29**, 659 (1994).
18. J.-L. Yue, Y.-N. Zhou, X. Yu, S.-M. Bak, X.-Q. Yang, and Z.-W. Fu, *J. Mater. Chem. A*, **3**, 23261 (2015).
19. H. Yoshida, N. Yabuuchi, and S. Komaba, *Electrochem. Commun.*, **34**, 60 (2013).
20. C.-Y. Yu, J.-S. Park, H.-G. Jung, K.-Y. Chung, D. Aurbach, Y.-K. Sun, and S.-T. Myung, *Energy Environ. Sci.*, **8**, 2019 (2015).
21. T. Shibata, Y. Fukuzumi, W. Kobayashi, and Y. Moritomo, *Sci. Rep.*, **5**, 9006 (2015).
22. A. J. Toumar, S. P. Ong, W. D. Richards, S. T. Dacek, and G. Ceder, *Phys. Rev. Appl.*, **4**, 064002 (2015).
23. M. D. Radin and A. Van der Ven, *Chem. Mater.*, **28**, 7898 (2016).
24. P. Vassilaras, A. J. Toumar, and G. Ceder, *Electrochem. Commun.*, **38**, 79 (2014).